Trends in Applied Sciences Research

ISSN 1819-3579

Academic
Journals Inc.

www.academicjournals.com

Trends in Applied Sciences Research 1 (3): 226-247, 2006
ISSN 1819-3579

Experimental Studies on Vibration Energy Transmission in Trapezoidal Corrugated Plates

Nirmal Kumar Mandal
Centre for Railway Engineering,
Central Queensland University, Bruce Highway,
Rockhampton, Queensland 4702, Australia

Abstract: Structural intensity technique is used to measure vibration power flow in technically or structurally orthotropic plates for flexural waves. The measurements are carried out in far-field conditions considering cross-spectra of acceleration in the frequency domain. Two trapezoidal corrugated plates are used. To investigate the effects of rigidity on flexural wave power transmission and vibration levels, an isotropic plate is also considered. The method of elastic equivalence is used to model the elastic properties of the corrugated plates so as to apply the classical orthotropic plate theory. It is observed that vibration power flow in trapezoidal corrugated plates is reduced compared to that of an isotropic plate used in this measurement. At the same time, it may be noted that the vibration response fields of trapezoidal corrugated plates are reduced compared to that of the isotropic plate. The geometrical modification for producing a trapezoidal corrugation, a passive method for controlling vibration, yields a good controlling method for noise, vibration and harness (NVH) problems in industries.

Key words: Structural intensity, flexural waves, trapezoidal corrugated plate, method of elastic equivalence, far-field conditions, flexural rigidity

Introduction

In engineering practice, flat plates are often reinforced by ribs, stringers, or corrugations. This method of stiffening is typically found in metal decking, roofing and sandwich plate cores, for example. The primary objective of this reinforcement is to enhance the flexural rigidity in one direction. The method of stiffening results in plates that are structurally anisotropic. Since most plates are rectangular and stiffeners or corrugations are aligned with the edges of the plates, the plates become structurally or technically orthotropic. This orthotropy is due to the form geometry, not due to the results of material properties. If the latter is true, the plate is called naturally orthotropic and its thickness must be uniform.

Machinery-induced vibrations are often a cause of concern or annoyance in such orthotropic structures in buildings, ships and air-craft and vibration control is therefore a topic of continuing study. In any such problems, the first approach is usually to modify sources and to isolate them from the surrounding structures via resilient vibration isolators. The vibration transmission characteristics of the structures between the sources and the area of unacceptable vibration levels must be examined and appropriate vibration control measures should be taken. It can be seen that from the vibration control point of view, there is a continuing interest in vibration isolation and structural vibration transmission.

Unwanted vibrations from a given source are controlled by varying the characteristics of mass, stiffness and damping. Engineers usually follow essentially three major approaches in solving noise and vibration problems (Andow *et al*., 1994):

- Reduction of overall vibration levels or vibration power flow at the design stages or post-production stages, by passive method, or modification of structures or mechanical systems
- Reduction of overall vibration levels using active vibration control methods such as feed forward control, pure feed back control and regenerative feed back control.
- Using a combination of the above with a hybrid system

The passive types, not requiring special driving power, are mechanically simple and are therefore widely used (Andow *et al*., 1994). With active and hybrid types where a weight is powered to generate a reaction force, adequate attention must be devoted to the effects of noise and vibration resulting from the driving apparatus of oscillators.

Several different methods of passive vibration control are available and each has its merits and demerits. Well-known passive control methods are: structural design, material selection, localized additions, artificial damping and resilient isolation for example (Mead, 1982). As fixed frequencies of excitation seldom occur, in the case of structural design, it is necessary to consider different frequencies and the resonant vibrations must be minimized. In the case of single force excitation, if the excitation is made to a nodal point, a mode cannot be excited. To minimize vibration levels, it is necessary that torsional stiffness of the structure should be low and flexural stiffness should be high. On the other hand, highest value of $E\eta$, product of Young Modulus and material loss factor of the material, gives lower vibration amplitudes under harmonic excitation at resonance. In the case of vibration transmission between the points on a structure, measurement of transfer function alone would not yield sufficient information to enable transmission paths to be identified. For this reason, an attempt has been made in recent years to develop methods for measuring vibration power flow through structures. Power flow concept can be seen to unify vibration control methods by seeking to minimize power input to the structures and then to minimize the power transmission through structures.

Ribs on plate-like structures change the structural stiffness and vibration response of the plate. Structural intensity mapping on a rib plate shows that vibration energy is flowing into the area where the rib is located (Mead, 1982) and acting as a sink. The rib is actually absorbing vibration energy. It is therefore necessary to investigate the vibration behaviors and estimate power flow through the form plates. Few attempts have been made so far to measure structural intensity and input power on corrugated plates, for example. In the following section, the development of structural intensity technique is presented chronologically.

Vibration intensity (structural intensity) technique has a unique aspect. It is not dependent on boundary conditions of the structures. This enables the investigation of the edge effects of vibration power transmission of pipes, plates and beams. But far- field power flow inherently contains some limitations in selecting measurement points. The measurement points should be away from the boundary and inhomogeneities of the plates. The effects of boundaries and inhomogeneities of the plates are called near field effects. The near-field effects decay exponentially as a function of position and extend to a distance of approximately half the bending wavelength from the boundaries and inhomogeneities of the plates (Noiseux, 1970). At low frequencies, the disturbing near-fields cover a large part of the plate and valid measurement could be made in the center region only. The far-field concept also enables the use of two sensors to determine an intensity vector at a point in any particular direction.

Most of the previous works undertaken on vibration power flow (structural intensity) were related to simple structures, typically beams and plates in flexure using the analysis both in time domain and frequency domain (Noiseux, 1070; Pavic, 1976; Verheij, 1980; Linjama *et al*., 1992; Bauman, 1994; Arruda *et al*., 1996). Some relevant works in composite materials using this idea are also available (Lam *et al*., 1989; Liew *et al*., 1989; Liew, 1992a,b; 1994). Using a most practical example, Lee and Kim (2004) employed this concept to quantify most dominant paths of vibration transmission in an outdoor compressor unit of an air conditioner.

Structural intensity can be computed numerically when predictions of structural behavior in various conditions are needed for complex build-up structures. Vibration intensity, generated by the interaction of dynamic stresses and vibration velocities, for beams and plates can be found by the finite element method (Garvic *et al*., 1993; Hambric *et al*., 1994; Hambric, 1995), by statistical energy analysis (Langley, 1992). The vibration power flow behaviors of a rectangular plate with stiffeners attached at various locations are investigated by Xu *et al*. (2005). The effects of geometric properties of the stiffeners on power flow are quantified. It is shown that injected and transmitted vibration power is dependent on the natural frequency and flexural rigidity.

Using power flow technique, vibration wave power was also formulated to single-layer naturally orthotropic plates both for general (Mandal *et al*., 2003) and far-field condition (Mandal *et al*., 2002) using flexural wave and for general conditions (Mandal *et al*., 2000) using quasi-longitudinal wave. In addition, the effects of flexural rigidity of different corrugated plates on damping loss factor were also quantified (Mandal *et al*., 2004).

Importance of vibration analysis and energy transfer on trapezoidal corrugated plates has drawn little attention in the recent years. Using an admissible deflection function incorporating the Rayleigh-Ritz method, a study of flexural vibration analysis was carried out in rectangular plates (Liew *et al*., 1990a) and skew plates (Liew *et al*., 1990b) and extended to trapezoidal plates for various end fixity (Liew *et al*., 1991), laminated trapezoidal composite plates (Liew *et al*., 1992), symmetric trapezoidal plates with linearly varying thickness (Liew *et al*., 1993) and unsymmetric trapezoidal plates of variable thickness (Liew *et al*., 1994).

Despite the progress made with respect to both methods and instrumentation, scope exists for further development as the analysis of vibration energy transfer generally had been in the areas of simple beams and thin plates. It is also seen from the literature survey that less work has been done relating to vibration power flow on orthotropic materials. Vibration power flow analysis in the area of orthotropic plates (corrugated plates) is essential for practical reasons. Beam stiffened plates, plate grid structures and corrugated plates are usually used in automotive, ship and aircraft structures. As this method gives a clear picture of locations of energy sources and sinks and quantifies energy transmission paths by employing vector maps, hence it essentially can be used for controlling noise and vibration in industry by incorporating proper damping treatments. Therefore any experimental research on orthotropic plates using structural intensity would give valuable information for controlling noise and vibration. The objective of this study is to use structural intensity technique as a measuring tool to investigate the influences of flexural rigidity of the trapezoidal corrugated plates on vibration transmission and its response. Consequently the effectiveness of geometric modification (passive control method) of plates for vibration energy control is quantified.

Input Power and Intensity

Power Input to a Point

The core of input power and vibration power flow was based on the imaginary part of

the cross-spectrum of two signals: between force and acceleration signals at input point for input power and between two acceleration or velocity signals at the measurement locations on the structure for vibration power.

In the frequency domain, total active power injected through a point junction by a point force is obtained as (Linjama *et al*., 1992)

$$P_i = \frac{1}{\omega} \mathrm{Im}\{G_{Fa}\} \tag{1}$$

Where, G_{fa} is the cross-spectrum of force and acceleration signals, Im is the imaginary part and ω (= $2\pi f$) is the angular frequency. If force is injected to a point on the plate in the direction perpendicular to the plane of plate, Eq. (1) could be valid for flexural waves. On the other hand, if it is injected to a point along the plane of the plate, the same Eq. (1) could also be valid for longitudinal waves. By putting the value of ω in Eq. (1), it is possible to get an input power equation in terms of frequency, f.

$$P_i = \frac{0.159}{f} \mathrm{Im}\{G_{Fa}\} \tag{2}$$

The imaginary part of the cross-spectrum of Eq. (2) could be achieved from FFT analyzer and by post-processing using Matlab or MS Excel, the input power P_i (W) could be computed. The Eq. (1) or (2) is valid for both isotropic and orthotropic plates.

Far-field Power

The idea of far-field power was first defined by Noiseux (1970). Approximately one-half of a flexural wavelength far from the edges and discontinuities of structures, the exponentially decaying near field components are negligible and the flexural wave field consists of free propagating waves. This idea is called far-field condition. The far-field condition simplifies structural intensity estimation. In isotropic plates, two components of active power from shear force (P_s) and moment (P_M) are equal (Noiseux, 1970). For isotropic plates, the far field power, also called time averaged power or active power, could be obtained as Linjama *et al*. (1992)

$$I = \frac{2\sqrt{Dm''}}{d\omega^2} \mathrm{Im}\{G_{12}\} \tag{3}$$

Where, I is the intensity (far-field power) in the direction of the transducer pair from 2 to 1 as in Fig. 1, d is the spacing of the accelerometers, D is the flexural rigidity of the plate, m'' is the mass per unit area of the plate, G_{12} is the cross-spectrum of acceleration signals, Im{} is the imaginary part. The Eq. (3) is applicable both in x and y directions of the plate (Fig. 1).

The imaginary part of the complex power, called reactive power, is defined as the standing wave power per unit width or it can be described alternately as that portion of the energy which resides in the stationary waves and is, essentially, stored within the medium (Quinlin, 1985).

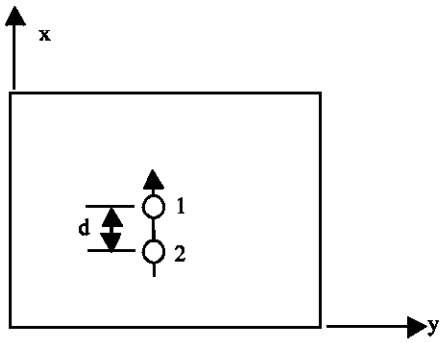

Fig. 1: Co-ordinate system of plate along with two-point transducer array

By normalizing the power flow at the far field conditions with respect to input power at a point source, power ratio, R, for the two transducer method could be found by taking the ratio of Eq. 3 to 1

$$R = \frac{2\sqrt{Dm''}}{d\omega}\frac{Im\{G_{12}\}}{Im\{G_{Fa}\}} \tag{4}$$

The flexural wave power in naturally orthotropic plates can be obtained using finite difference approximation. Recently, a measurement method to quantify power flow in naturally orthotropic plates has been developed (Mandal *et al*., 2002). This model is indicating power transmission in x-direction of the plate and is presented below as

$$I_x(f) = \frac{2\sqrt{D_x m''}}{d\omega^2} Im\{G_{12}\} \tag{5}$$

where G_{12} is the cross-spectrum of the acceleration signals at points 1 and 2, D_x is the flexural rigidity of the plate in x-direction. This relation presents the flow of vibration power in orthotropic plates in the x direction from point 2 to 1 (Fig. 1). The y-component of this power could be obtained by interchanging the x and y axes in the Eq. 5 leading to

$$I_y(f) = \frac{2\sqrt{D_y m''}}{d\omega^2} Im\{G_{12}\} \tag{6}$$

The cross-spectrum of two acceleration signals could be measured directly by multi-channel FFT analyzer using two accelerometers. An estimate of it can, however, be found using the frequency response method with one transducer technique (Linjama *et al*., 1992). As a result phase errors are reduced. Only one cross-spectrum of acceleration signal is required to obtain total power.

Experiements

The objective of this experiment is to measure vibration power transmission in technically orthotropic plates. Trapezoidal corrugated plates, one small and one big, are considered. In addition,

Table 1: Physical dimensions of one repeating section of trapezoidal corrugated plate

	Trapezoidal corrugated plates	
Types of plate/Physical quantities	Small	Big
Length of one repeating section, d_1 in mm	90.0	150
Actual flat length of one repeating section, s in mm	111.6	232
Number of repeating sections	10.0	6

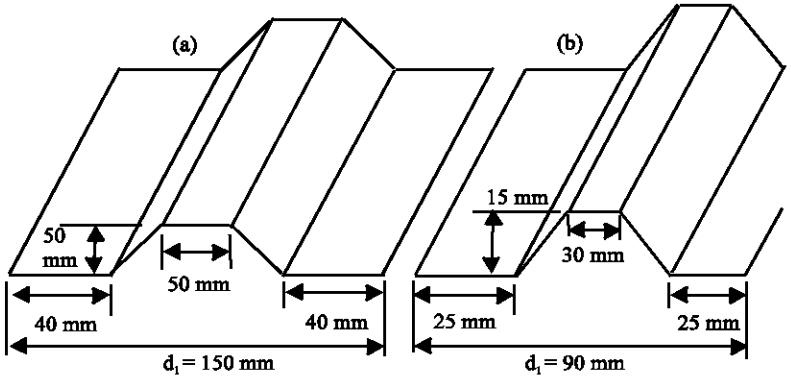

Fig. 2: Physical dimensions of one repeating section of trapezoidal corrugated plates (a) for big corrugated plate, (b) small corrugated

one isotropic plate of steel is also used for investigating the effect of flexural rigidity on power transmission by comparing the results. This observation is further supported by measuring the frequency response function of acceleration of all the plates. The shape and size of the corrugated plates are shown in Table 1, Fig. 2, 4 and 5 and how this technical orthotropy resulted is discussed earlier.

The classical plate theory for isotropic plates must be modified to account for this orthotropy. The response of such plates is described analytically by the theory of orthotropic plates (Troitskey, 1976; Timoshenko, 1959; Ugural, 1981) provided that the rib and corrugated plates are accurately modeled as equivalent homogeneous orthotropic plates (naturally orthotropic plates) with uniform thickness by defining properly their different elastic constants. As these elastic constants are required to estimate vibration power flow in plates, an accurate determination of these is important. These elastic constants together with plate geometry, density and boundary conditions of the plate play an important role for its dynamic response. If possible, the elastic constants should be determined experimentally. Since such testing is not always possible, a reasonable approximation of plate rigidity is required. Method of elastic equivalence (Troitskey, 1976; Timoshenko, 1959; Ugural, 1981; Huffington *et al*., 1956; Blackketter *et al*., 1989; Szilard, 1973) is generally used to replace the structurally orthotropic plate with the equivalent naturally orthotropic plate of uniform thickness. The trapezoidal corrugated plates in this study are modeled to naturally orthotropic plates by the method of elastic equivalence so as to apply orthotropic plate theory.

The characteristic dimension d_1, the length of one repeating section and s, the actual flat length of both trapezoidal corrugated plates are shown in Fig. 2 and its characteristic dimensions are also shown in Table 1. Both corrugated plates are made from an isotropic plate but the technical or structural orthotropy results from the modification of geometry of the isotropic plate. When the actual

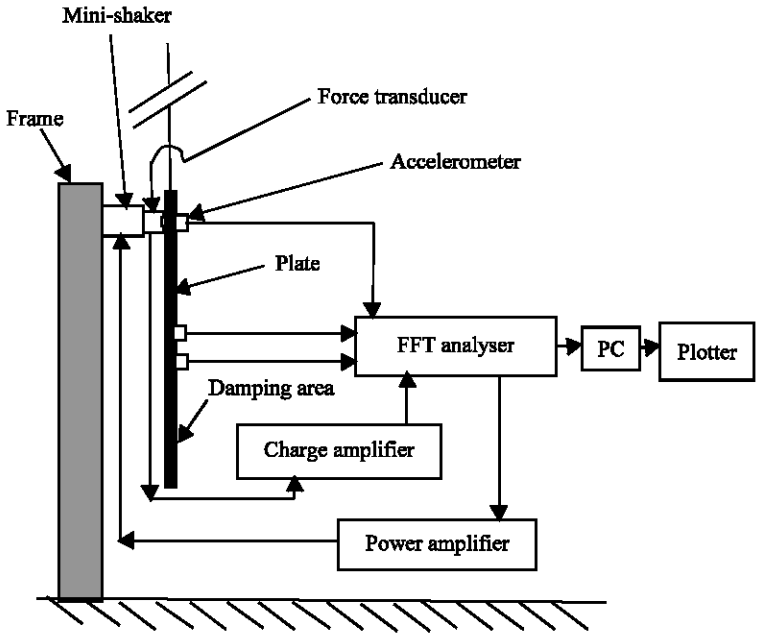

Fig. 3: Test rig and instrumentation of a freely suspended plate excited by a mini-shaker at one end and heavily damped at the other end, indicating the locations of force transducer and different accelerometers (input and far-field)

trapezoidal corrugated plates are transferred to equivalent plate, there would no change of plate dimension (size) and thickness would be the same as that of the isotropic plate (Ammar, 1973).

Instrumentation, Data Acquisition and Processing

A laboratory test rig was constructed for experiments. The schematic diagram and instrumentation for the measurement of flexural wave power on a steel isotropic plate and trapezoidal corrugated plates were fabricated as in Fig. 3. At the upper end of the plate, a mini-shaker (B and K type 4810) was used to provide random white noise excitation to the plates through a force transducer (B and K type 8200). Two accelerometers mounted away from the source and boundaries were used to measure far-field power. The major components of instrumentation were the miniature accelerometers (piezoelectric, ICP, with an effective mass of 1.7 g) and a multi-channel FFT analyzer (HP 35670A). The accelerometers were mounted on the plate with beeswax. The mini-shaker was driven by internal noise source of the FFT analyzer. The Standard Data Files (SDF) of the measurement were transferred from analyzer to a PC for post processing. As required by Eq. 2 and 5 for input power and intensity respectively, cross-spectrum between force and acceleration at input point and the same between two acceleration signals are measured by FFT analyzer. The constant parameter and frequency term are incorporated with cross-spectrum to get input and far-field power. The post processing is carried out using Excel.

The sides of all plates (Fig. 4) are 0.90 m and the thickness of the isotropic plate and equivalent corrugated plates is 0.8 mm. The material properties such as Young's modulus and Poisson's ratio are 162.8 GPa and 0.31, respectively. With these plate dimensions and material properties, it can be

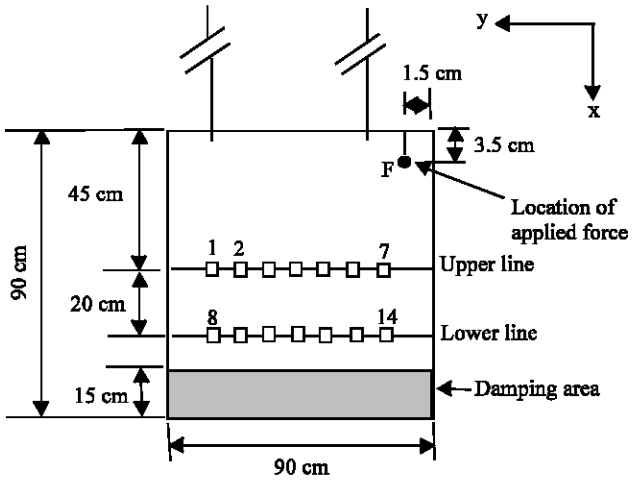

Fig. 4: Different measurement points on two measuring lines (seven on each line), indicating locations of applied force and damping on plate

expected that the far-field condition (at least half a wavelength from the boundaries and source) is at the center of the plate at frequencies from about 9.12 Hz upwards. The upper frequency limit for flexural wave condition to be valid (wavelength equal to six times the thickness of the plate (Cremer and Heckl, 1988) was 320.7 kHz. The spacing of the accelerometer positions should be as short as possible so as to minimize finite difference error, but too short a distance causes phase mismatch error. The spacing, d, was chosen rather arbitrarily to be 20 mm. The spectral bandwidth was set at 800 Hz. At the upper frequency limit of 800 Hz, the wavelength was calculated to be 96.10 mm for Isotropic Plate (IP). For Small Trapezoidal Corrugated Plate (STCP) and big trapezoidal corrugated plate (BTCP) the flexural wavelengths are respectively 520.34 and 931.06 mm. The calculations of wavelength are presented in Appendix A. Thus the accelerometer spacing is approximately 1/4.8 of the wave length for IP, 1/26 for STCP and 1/46 for BTCP.

All plates were freely suspended vertically using steel strings at two points and the lower part was damped heavily by spongy-foam and sand (Fig. 4). This type of damping is usually provided at the end of the test object to suppress the reflections. Other substances used for this purpose are plastics, adhesive tape sheet and similar items. The effectiveness of damping materials was tested by measuring the response of the plate with or without the use of damping materials. Vibration fields without damping materials would result in a reverberant plate as vibration energy reflects back and forth in the plates. A more stable response was observed when the measurement was taken with damping materials. This ensures that a reverberation condition was less obvious. Such type of measurement to ensure effectiveness of damping material can be found in literature (Zhang and Mann, 1996). Similar measurement using sand as end damping material was also undertaken.

Suspension of trapezoidal corrugated plates needs careful attention so as to make x-axis parallel to the direction of corrugation (Fig. 2). As a result the flexural rigidity in x-direction of the plates, D_x, is greater than that of D_y. In every plate, like isotropic, two measurement lines were considered where different points were located as shown in Fig. 4. Only a small change was made for the measurement of energy transfer in the big trapezoidal corrugated plate. This was due to its different characteristic

Table 2: Different significant dimensions relating to measurement of all plates

Plates/Parameters	IP	STCP	BTCP
Distance between measurement points (mm)	90	90	75
Distance of extreme points to the edge (mm)	180	180	225
Measurement lines	2	2	2
Number of points	14	14	14

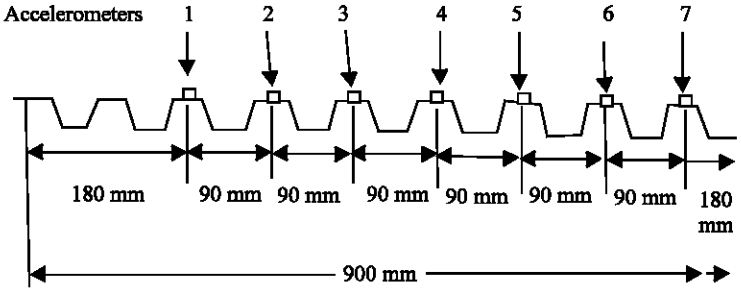

Fig. 5: A sketch of a region of cross-section of STCP, showing 7 accelerometers in one measurement line, distances between the accelerometers and distance of far-end accelerometer to the edge of the plate (not in scale)

dimension d_1. The distance between the measurement point and the distance of extreme points to the nearest edges of the plates are given in Fig. 5 and Table 2.

The suspension and force injection were carefully tested in order to minimize the generation of vertical and torsional motion of the plates which could disturb the true detection of lateral horizontal motions. A calibration test of the entire measurement chain was undertaken before the actual measurements. The key components of these measurements, such as force transducer, accelerometer and others, were tested and calibrated separately. Repeatability was checked and errors were less than 2% in the frequency range of interest.

In the measurement of narrow band FFT modes, windowing is the most important part of data acquisition in the frequency domain. In these measurements, a Hanning window was selected. The Hanning window produces narrow spectral lines and so it is useful for accurate measurements. It is the most generally used window because it gives a good trade-off between frequency resolutions and amplitude accuracy. The Hanning window gives a better solution of leakage. Windowing, however, does slightly alter the data records, but does result in a vast improvement in measurement of data that is not periodic in time domain.

In the measurements, mainly the imaginary part of cross-spectrum between two accelerometers' signals at the far-field (as required by Eq. 5) and the same between force and acceleration at the excitation point (as required by Eq. 2) was measured. The mini-shaker, providing random white noise, was connected to the internal noise source of the FFT analyzer. White noise commonly known as random excitation is constant in magnitude over the frequency range. For the measurements of cross-spectrum between two acceleration signals for all fourteen points in the far fields (Fig. 4), a fixed array of transducers (two accelerometers at a 'd' distance apart, Fig. 1) was used for all points rather than moving a transducer sequentially between the locations of the accelerometer for measurement point. In the case of one transducer arrangement, a stationary field should be made during data acquisition of cross-spectral. Additional transducer for two-transducer measurement exerts a negligible

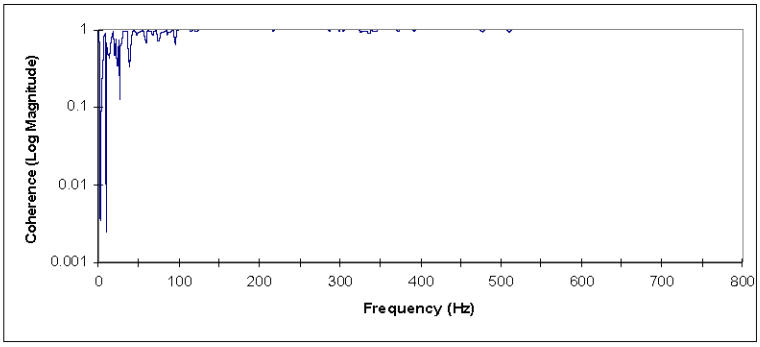

Fig. 6: Coherence function between force and acceleration at the input point for isotropic plate, spectral resolution of 1 Hz

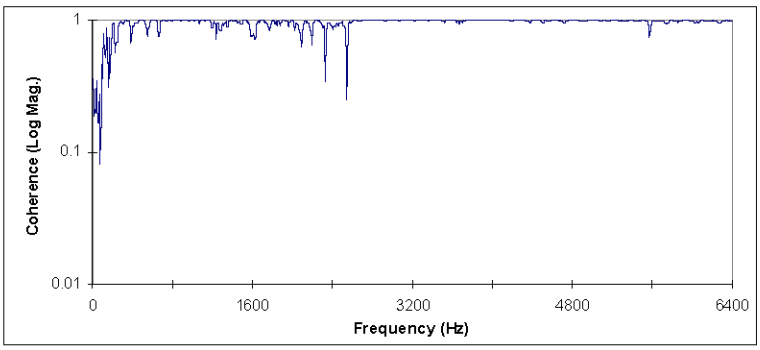

Fig. 7: Coherence function between force and acceleration at input point for STCP, resolution of 8 Hz

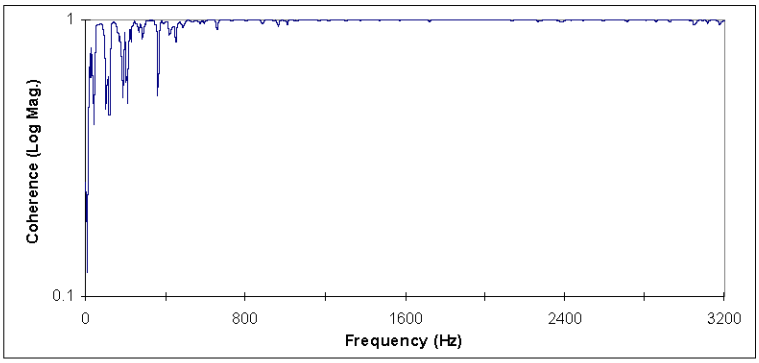

Fig. 8: Coherence function between force and acceleration at input point for BTCP, resolution of 4 Hz

local disturbance as the mass of the transducer is small. Investigation of the local influence on vibration field is beyond the scope of this study. The FFT analyzer was used to collect 200 ensemble averages of the cross-spectra, auto-spectra and coherence functions needed in the subsequent processing.

An example of coherence functions observed during data acquisitions in steel isotropic plate is shown in Fig. 6 with the frequency resolution of 1 Hz. Some lack of coherence occurred at the low frequencies and it was deemed to be acceptable on overall basis (Linjama *et al*., 1992). A more sufficient spectral resolution may improve coherence values at these frequencies. Similar nature of coherence function is found in the case of STCP (Fig. 7) and BTCP (Fig. 8). In both cases, a larger frequency bandwidth was considered with spectral resolution of 8 and 4 Hz respectively. FFT analyzer (HP 35670A) having maximum resolution lines of 800 was considered for these coherence measurements.

Results

In this study, both input power injected to a point and far-field power of the plates were measured. The same force signal was applied throughout the experiments for all the plates and was monitored. This same force signal was provided by maintaining same setting and level of internal source of FFT analyzer. This enables the comparison of far-field power between isotropic plates and corrugated plates to investigate the influence of flexural rigidity on power transmission. The imaginary part of the cross-spectrum of force and acceleration at input and the imaginary parts of cross-spectrum between two acceleration signals at various measurement locations (Fig. 4) were used respectively to compute input power and far field power using the Excel program.

For flexural wave power measurement, input force was injected to a point (Fig. 4) on the plates in the direction perpendicular to the plates. The location of input force was chosen at the top corner of the plate so as to observe more intensity field at distinct frequencies of resonant and non-resonant character. The excitation force signal was random white noise, given by the internal noise source of the FFT analyzer used, in the frequency range of 0 Hz to 800 Hz as in the Fig. 9. A stable constant magnitude of force (N) is observed throughout the frequency range.

Measurement of vibration intensity on beams can usually be performed by inserting transducers in a four-point or two-point array in one location. But one location measurement results in very raw information of energy transmission in case of the plates. Vibration is generally measured on a random

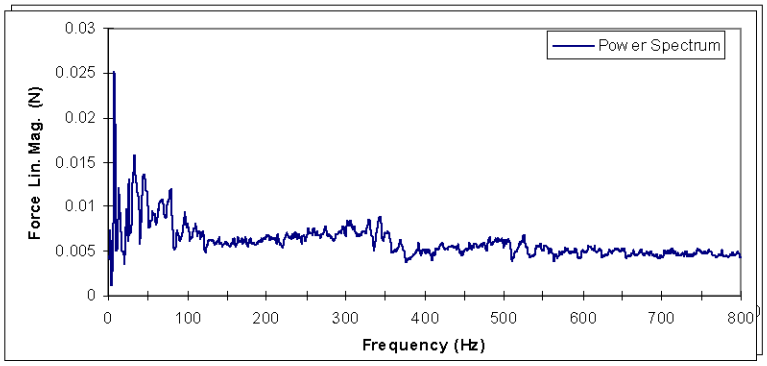

Fig. 9: Random force signal for low frequency range measured by force transducer

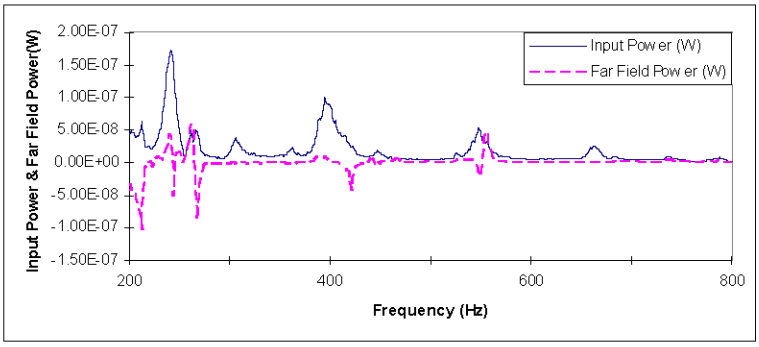

Fig. 10: Normalized far-field power and input power for STCP from upper measurement line, spectral resolution of 1 Hz

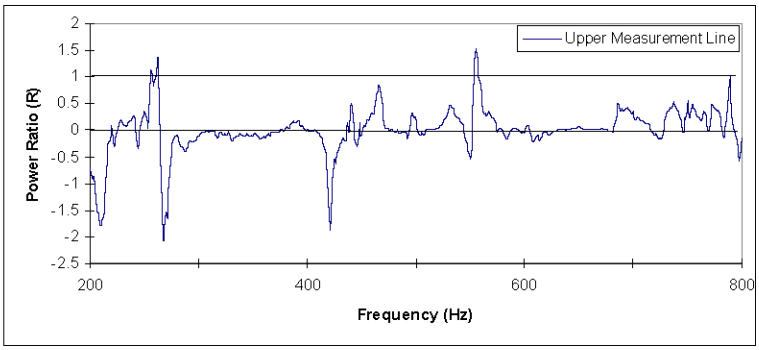

Fig. 11: Power ratio of far-field power and input power for STCP, spectral resolution of 1 Hz

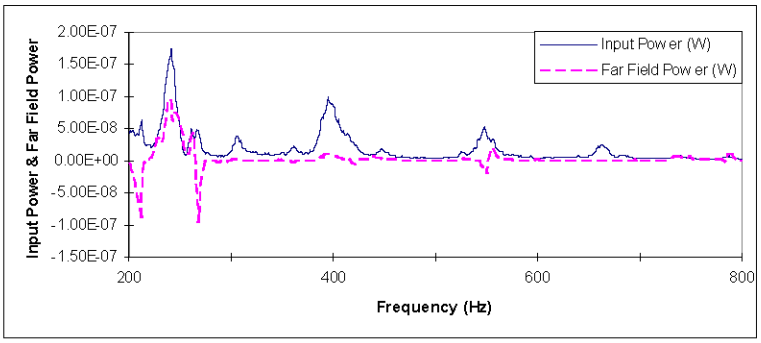

Fig. 12: Normalized far-field power and input power for STCP from lower measurement line, spectral resolution of 1 Hz

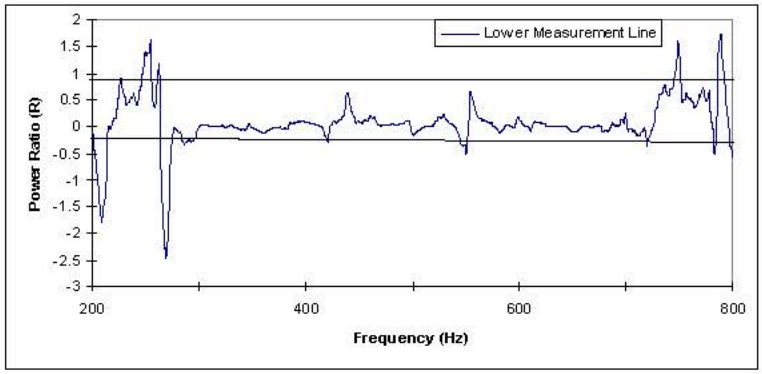

Fig. 13: Power ratio of far-field power and input power for STCP, spectral resolution of 1 Hz

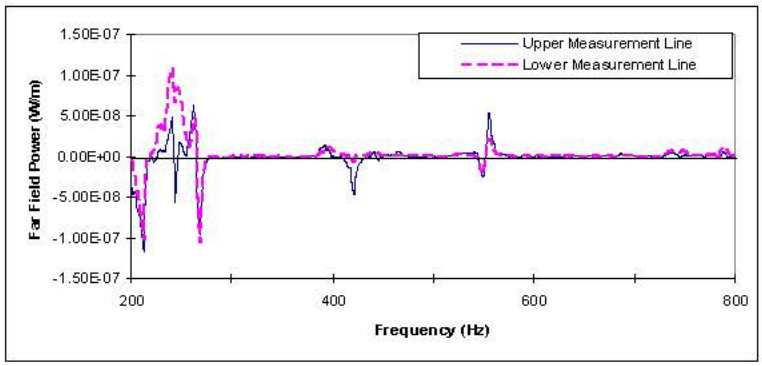

Fig. 14: Relative far-field power flow for STCP from both measurement lines, spectral resolution of 1 Hz

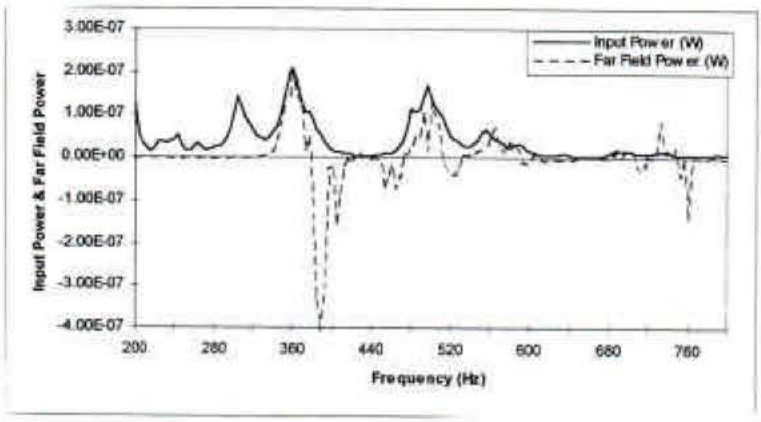

Fig. 15: Normalized far-field power to input power for BTCP from upper measurement line, spectral resolution of 4 Hz

point grid or perpendicular to different lines (Fig. 4) on the plates (Linjama, 1994). Estimates for net power through the measurement line grid were constructed as a line integral (by calculating the average) of the normal components of the properly scaled intensity vectors. Total power transferring through a line grid could be obtained as

$$I_{total} = \int_{L} \vec{I} \bullet \vec{n}\, dL \tag{7}$$

Where $\vec{I}$ is the intensity vector and $\vec{n}$ is the unit normal vector perpendicular to the line. Average power could be computed from total power taking into account the number of measurement points on each line (Fig. 4). Proper scaling of the intensity vector is necessary due to the fact that the units of input power and intensity are W and W/m respectively (Linjama *et al*., 1992). When intensity is compared with input power, it is necessary to normalize both in the same unit. In this measurement, the intensity vector is properly scaled to the same unit of input power (W) when both are normalized.

Input power and far-field power for an isotropic plate and both for small and big trapezoidal corrugated plates were estimated. The far-field power was normalized to input power to facilitate comparison of the results and the method. This is possible because the same measurement state was used for all plate models for input force to ensure a constant and repeatable condition. For STCP, Fig. 10 and 12 show normalized far-field power to input power, Fig. 11 and 13 for power ratio, R and Fig. 14 for far-field power from two measurement lines. For BTCP, on the other hand, the same method was used for data acquisition and analysis. Spectral resolution was increased to 4 Hz for calculation of energy transfer. The reason for higher spectral resolution is because different resolution lines of 200 were considered to make it different from that of STCP. Figure 15 shows normalized far-field power to input power for this plate.

Discussion

Measurement of Structural Intensity

The measurement method applicable for naturally orthotropic plates is used in this experimental study to verify the soundness of the method for flexural waves. Naturally orthotropic plates' thickness is uniform. Different orthogonal rigidity occurs due to different material properties (E and υ) in different directions. It is not due to geometric modification as in the case of technical orthotropy. There is no necessity to use the method of elastic equivalence with naturally orthotropic plates. The far-field energy transfer model (Mandal *et al*., 2002) can be used directly in these plates. But the method cannot be applicable to structurally orthotropic plates because thickness of the plates is not uniform. So as to apply the model (Mandal *et al*., 2002) to the plates, the method of elastic equivalence is considered. The far-field power flow model as applicable to naturally orthotropic plates could be used on structurally orthotropic plates with reasonable accuracy (Szilard, 1973). Hence it is also possible to investigate usability of elastic equivalence. Trapezoidal corrugated plates are used for this purpose. Shape and size of all these plates are presented in the previous section. The corrugated plates are considered in this study because these types of plates are widely used in industrial applications.

The standard way of providing the soundness of any method and technique in structural intensity is to normalize vibration power transmission in structures to input power injected into it (Linjama *et al*., 1992; Bauman, 1994; Mandal *et al*., 2005). Under all conditions, it is expected that input power must be greater than the vibration power flowing (Linjama *et al*., 1992) for identical conditions on the same structure. In the case of orthotropic plates, far-field power was normalized to

the input power injected to these plates for facilitating comparison of the results. From Fig. 10 and 12, it is observed that input power has mostly higher values than those of far-field power for STCP. This is confirmed by Fig. 11 and 13 where power transmission is plotted in ratio form (far-field to input). In some cases, far-field power may however exceed the input power and power ratio between far-field power and input power on the same plate is greater than unity (Linjama *et al*., 1992; Bauman, 1994). In Fig. 15, for BTCP, a similar pattern of power flow transmission is observed. It is further important to note that in some frequencies, negative values of far-field power were detected (Fig. 14 and 15) and thereby power ratio became negative. However, the characteristics of the results are consistent with the results reported in the literature (Linjama *et al*., 1992; Bauman, 1994). The plots of power ratio, R of these plates (Fig. 11 and 13) ensure this nature in a more convenient way. In the region closer to the damping area (lower measurement line), reflections of wave are less, with strong power flow as expected in the direction towards the damping area (Fig. 14).

These two aspects of vibration power flow may be explained by the following idea.

Three types of power flow pattern (Tanaka, 1996) are observed: straight type, S-shaped type and vortex type. Among them, S-shaped type and vortex type flow pattern may play important roles for energy transfer. These patterns are also applicable to in-plane waves. This is also true for acoustic intensity (Tanaka, 1996). The use of more measurement points on a measurement line (Fig. 4) may resolve this anomaly. Reflections and scatterings of waves from edges of the plates (only the lower side of the plates is damped) and rotational (vortex) characteristics of power flow field create additional influence on far-field power which can cause it to be greater than input power and yielding negative values.

Another clue regarding the reason for this discrepancy of vibration power exceeding the input power is that it may be due to the number of measurement points considered. Vibration power transmission in plates (Eq. 7) is obtained by averaging the normal component of intensity vector (structural intensity) perpendicular to the line (Fig. 4). But there are seven measurement points on each line grid. Using a few more measurement points on each line and averaging the vibration power crossing through these points may solve this problem. A consideration of too few measurement points on a line results in loss of valuable frequency components. However, this is a usual practice for plate vibration measurement (Linjama 1994).

Passive Controlling Method

In this research, both vibration power and vibration amplitude of corrugated plates are compared with that of the isotropic plate. This type of comparison for STCP model is shown in Fig. 16. A valid comparison of the effects of rigidity on energy transfer is ensured as the same input excitation was provided to all plates. From this figure, it is shown that vibration power flow is reduced in the case of corrugated plate in comparison to that of isotropic plate. A more fruitful comparison would, however, be possible by plotting the values of far-field power ratio for different plates (Fig. 17). The ratio of far-field power of STCP and isotropic plate is mostly less than unity except for some frequencies. The value of flexural rigidity for isotropic plate (7.684 N-m) was less than the rigidities of corrugated plates (7922.93 Nm for STCP and 97.76×10^3 N m^{-1} for BTCP) (values of flexural rigidity for different plates are illustrated in appendix A). From these Fig. 16 and 17, it is observed that with the increase of flexural rigidity, vibration power flow reduces. Frequency Response Function (FRF) of acceleration of STCP and BTCP is reduced to that of the isotropic plate. Higher stiffness enhances more damping, thereby amplitude of vibration reduces (Fig. 18 and 19) and structural intensity does too (Fig. 10 and 12). Only for a few frequencies is the vibration response of isotropic

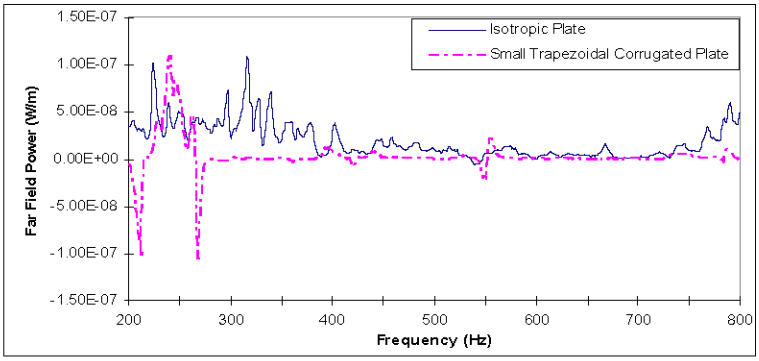

Fig. 16: Comparison of far-field power for Isotropic Plate (IP) and STCP from lower measurement line

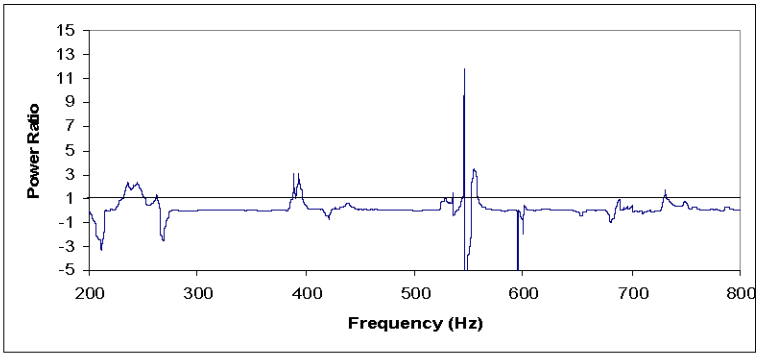

Fig. 17: Power ratio of far-field power of STCP to Isotropic Plate (IP) from lower measurement line

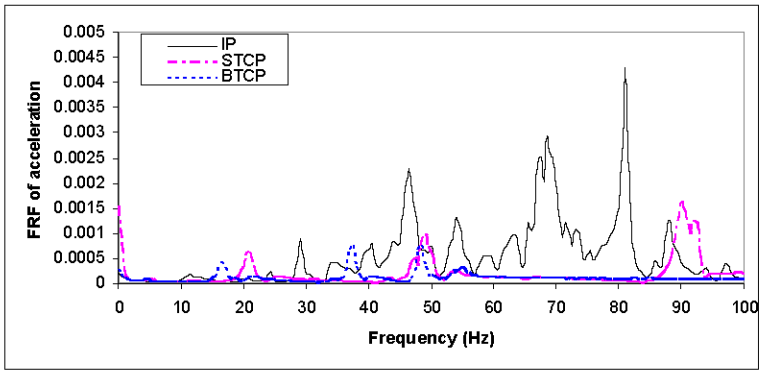

Fig. 18: Comparison of Frequency Response Function (FRF) of acceleration of Isotropic Plate (IP), STCP and BTCP, spectral resolution of 1 Hz

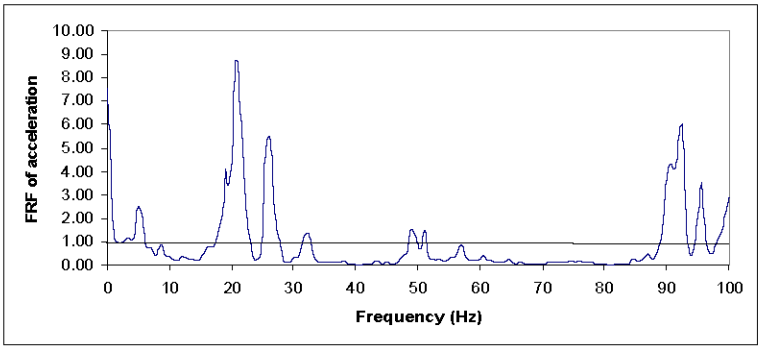

Fig. 19: Ratio of FRF of acceleration of STCP to Isotropic Plate (IP), spectral resolution of 1 Hz

plate less than that of corrugated plates (Fig. 18 and 19) and the ratio of FRFs (trapezoidal to isotropic plate) greater than unity. This is because of resonance vibration responses of the corrugated plates; vibration response at resonance is larger compared to that of other frequencies and it can be greater than the response of isotropic plate. However, on an overall basis, it may be argued that vibration responses are reduced for corrugated plates.

This research provides this distinct means of controlling flexural waves in structures. Other than controlling of vibration sources by isolating them from the structure, a passive method of controlling them by increasing flexural rigidity of the structures gives a better way not only to reduce vibration amplitude but also to reduce vibration energy transfer through plates. As higher rigidity of plates ensures more damping, more vibration energy is absorbed in the plates resulting in less acoustic power radiation into the surroundings. The effect of temperature rising as a result of absorption of energy due to corrugation has not been investigated in this study.

The outcome of reducing vibration power flow and vibration amplitude with the increase of flexural rigidity, a passive means, could ensure an efficient way to control noise and vibration in industrial applications. The increase of flexural rigidity by corrugation of the plates does not result in any major increase in mass of the plate. To achieve the same amount of stiffness increase by increasing thickness of the plate or stiffening with other beams would surely yield more mass of the plate than by use of the corrugation. Corrugation of plate is therefore an effective controlling method of vibration power and vibration amplitude for flexural waves. Effects on rigidity of sinusoidal and other types of corrugation require more attention now to investigate its influence on vibration energy transfer by flexural waves and in-plane waves.

Through literature search on vibration power flow, it is evident that the measurement models for vibration power flow have been developed mainly for simple structures. Structural intensity is, however, applicable to naturally orthotropic plates (Mandal *et al*., 2002). But no method has been found so far which is applicable for experimental investigation in technically or structurally orthotropic plates. Therefore, a method of elastic equivalence was employed to corrugated plates to use the far-field method (Mandal *et al*., 2002). This is another objective of this study to investigate the effectiveness of method of elastic equivalence. The similarity of far-field power transmission for the same input forcer when comparing isotropic plate (without elastic equivalence) and orthotropic plates (with elastic equivalence) would certainly ensure the soundness of the method of elastic equivalence.

Rather than using elastic equivalence for estimating vibration power transmission in corrugated plates, the Finite Element Method (FEM) and the Statistical Energy Analysis (SEA) may be used to verify experimental investigation.

Accuracy in Measurements

Errors in measurements are quite inherent. Good measurement method and instrumentation give results of higher accuracy, but provide the results at least close to the true value of power flow measurements. It is stated before that the spacing of 20 mm between the sensors was chosen rather arbitrarily. Relationship of spacing and wavelength were stated before. It is presented further in Table 3 to enhance discussion on errors of measurements. The ratio of spacing to bending wavelength should be 0.2 for upper frequency limit and 0.15 for lower frequency limit (Key *et al*., 1996). The use of this spacing criterion provides an optimal trade off between the reduced finite difference errors afforded by small sensor spacing and reduced sensitivity to standing wave related errors afforded by larger sensor spacing. The finite difference errors start to appear if the spacing is greater than 1/5 of wave length (Linjama *et al*., 1992). The ratio of spacing to wavelength of this study ensures good accuracy in terms of finite difference errors. On the other hand, this ratio between the spacing and the wavelength, because of not providing larger sensor spacing, gives some phase mismatch of the sensors due to standing waves. Thus it may provide some phase mismatch errors. It was stated before that the end damping ensured plates with fully propagating waves, suggesting the reactive and reverberant energy was not disturbing. It may thus be reasonably assumed that phase error does not play a significant role. If the reverse were true, phase error cancellation property of the frequency response technique would be employed (Linjama, 1994). Phase mismatch errors may further occur due to amplitude and imperfect positioning of sensors. It could be quite large if the coherence values are not close to unity and /or if a large number of averages of samples are not taken (Linjama, 1994). In this study, it was observed that all the coherence values (Fig. 6-8) are very close to unity except in some initial frequencies. On the other hand, a quite large number of averages (200) were considered. It could therefore be expected that the error due to phase mismatch would be marginal. Random errors arise due to fluctuation (in either direction) of measurement. Systematic (bias) errors, by contrast, evolve due to improper transducer arrangement (not change). Systematic errors can be studied through inter-comparisons, calibrations and error propagation. The investigation of finite difference, random and bias error is beyond the scope of this study. However, this is a major challenge for vibration engineers and scientists to achieve an instrumentation technique of measuring structural intensity with minimum acceptable errors. Useful suggestions in this direction are given by Shibata (1994). If strong end damping is provided for both lower and vertical sides of the plate for a greater region, fully propagating waves may exist in the measurement region. As a result, measurement error would be reduced more.

Problems of precise intensity measurement sometimes occur due to the complex shape of corrugation of the plates. The near-field effects decay away from boundary ($\lambda/2$ wavelength away). Therefore measurement location would be in the middle region of the plates. For complex geometry of structures like trapezoidal corrugated plates, measurement along the corrugation (x-axis) is considered to be simpler compared to that in the direction perpendicular to corrugation (y-axis). The method of elastic equivalence, used in this study, modifies the complex cross-section of trapezoidal

Table 3: Ratio of spacing of transducer and wave lengths of the plates

Ratio/Plates	Isotropic plate	STCP	BTCP
Spacing/wavelength	1/4.8	1/26	1/46

corrugated plate to a simple plate of uniform thickness. Therefore, the question of facing different geometry in measurement is not evident. Consequently, it may be argued that the results of measurements can be trusted.

Conclusions

In this study, an experimental investigation is carried out to find the effects of flexural rigidity on flexural wave power flow. For this purpose, two trapezoidal plates are used. One isotropic plate is also used for comparison. The trapezoidal corrugation is produced by due to a geometric modification of an isotropic plate and as a consequence, flexural rigidity in one direction is increased significantly.

Some FRFs of acceleration for all plates are presented to show the effects of rigidity on vibration response. It is observed that due to the increase of flexural rigidity, both vibration power flow and amplitude are reduced. As a result, it may be argued that the structural design, increasing the flexural rigidity by modifying its geometry, is an effective passive method for noise and vibration control in industries. Increase of rigidity by corrugation does not yield much weight penalty as compared to other methods. By increasing thickness of the plates, similar amounts of reduction in vibration transmission and response are possible, but this results in additional cost and mass of the plates. In addition, increasing flexural rigidity does not require additional sensors/actuators as is required for active vibration control such as feed forward, feed back and similar others.

Appendix A

Calculation of Flexural Wave Lengths for Different Plates

Calculation of flexural wave length for plates requires values of material properties such as Young's Modulus, Poisson's ratio and other dimensions such as thickness, length of repeating section (d_1), mass per unit area (m''), flexural rigidity of the plate and frequency. The basic equations for calculation of flexural wave length are given below:

$$k = \sqrt[4]{\frac{\omega^2 m''}{D_x}} \tag{A1}$$

$$\lambda = \frac{2\pi}{k} \tag{A2}$$

where k is the flexural wave number, ω is the angular frequency, λ is the flexural wave length and D_x is the flexural rigidity of the corrugated plates in the x-direction. If D_x is replaced by D, the flexural rigidity of the isotropic plate (IP), the Eq. A1 could be useful for isotropic plates. From Eq. A1 and A2, the final form of flexural wave length equation could be manipulated as

$$\lambda^2 = \frac{2\pi}{f}\sqrt{\frac{D_x}{m''}} \tag{A3}$$

where, f is the frequency of the analysis. To calculate D_x for corrugated plates, it is necessary to evaluate the position of neutral axis (Fig. A1) and moment of inertia (I) about its neutral axis

Table A1: Table for flexural wave lengths for different plates, one isotropic plate and other two trapezoidal corrugated plates

Types of plate	Neutral axis (mm)	D_x or D (Nm)	λ (mm) for 800 Hz
I P	0	7.684	96.10
STCP	6.75	7922.93	520.34
BTCP	22.56	97.76×10^3	931.06

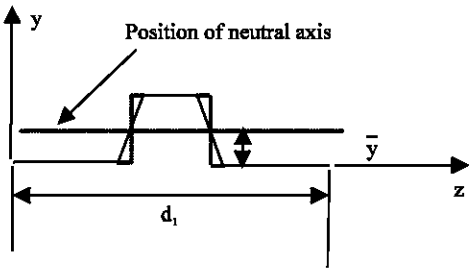

Fig. A1: Position of neutral axis of one repeating section of trapezoidal corrugated plate, indicating co-ordinate system

(Mcfarland, 1967). Mcfarland, (1967) analytically derived the flexural rigidity in x and y directions of rectangular corrugated plate. These are given by the following relations:

$$D_x = \frac{E\, I_x}{d_1} \tag{A4}$$

$$D_y = \frac{E\, t^3 d_1}{12\, s} \tag{A5}$$

where, E is Young's Modulus of the material and t is the material thickness, d_1 and s are the characteristic dimensions of corrugation, defined before. For trapezoidal corrugated plates in flexure, such analytical models are not however developed so far. Consequently, a modeling technique (Ahmed, 1996) is necessary to convert trapezoidal corrugation to rectangular corrugation (Fig. A1) so as to apply the relations (A4) and (A5).

Table A1 shows the related information for flexural wave length of the plates.

References

Ahmed, E., 1996. Behavior of profile steel sheet dry board panel, M.Sc. Thesis, UKM, Malaysia.

Ammar, A.B., 1973. Analysis of light gauge steel shear diaphragms, Ph.D Thesis, Cornell University, USA.

Andow, K., A. Minemura, Y. Yokokura and Y. Murata, 1994. Cut off characteristics of structure-borne sound caused by hybrid damper. Inter-noise, 94: 713-716.

Arruda, J.R.F. and J.P. Campos, 1996. Experimental determination of flexural power flow in beams using a modified prony method. J. Sound Vibrat., 197: 309-328.

Bauman, P.D., 1994. Analytical and experimental evaluation of various techniques for the case of flexural waves in one-dimensional structures. J. Sound Vibrat., 174: 677-694.

Blackketter, D.M. and A.P. Boresi, 1989. Cross ribbed rectangular plates. Mech. Struc. Mech., 17: 321-331.

Cremer, L. and M. Heckl, 1988. Structure-Borne Sound: Structural Vibration and Sound Radiation at Audio Frequencies, Springer-Verlag, Berlin.

Gavric, L. and G. Pavic, 1993. A finite element method for computation of structural intensity by the normal mode approach. J. Sound Vibrat., 164: 29-43.

Hambric, S.A. and P.D. Taylor, 1994. Comparison of experimental and finite element structure-borne flexural wave power measurements for straight beam. J. Sound Vibrat., 170: 595-605.

Hambric, S.A., 1995. Comparison of finite element prediction and experimental measurements of structure-borne power in a T-shaped beam. Proc. Inter-noise, 95: 685-688.

Huffington, Jr. N.J. and V.A. Blackburg, 1956. Theoretical determination of rigidity properties of orthogonally stiffened plate. J. Applied Mech., Trans. ASME, pp: 15-20.

Kay, K.Q. and D.C. Swanson, 1996. Error in bending wave power measurements. Noise Control Eng. J., 44: 185-192.

Lam, K.Y., L.M. Liew and C.T. Chow, 1989. Study on flexural vibration of triangular composite plates influenced by fibre orientation. Composite Structures, 13: 123-132.

Langley, R.S., 1992. A wave intensity technique for the analysis of high frequency vibration. J. Sound Vibrat., 159: 483-502.

Lee, H.J. and K.J. Kim, 2004. Multidimensional vibration power flow analysis of compressor system mounted in outdoor unit of an air conditioner. J. Sound Vibrat., 272: 607-625.

Liew, K.M., K.Y. Lam and S.T. Chow, 1989. Two-dimensional orthogonal polynomials for vibration of rectangular composite plates. Composite Structures, 13: 239-250.

Liew, K.M., K.Y. Lam and C.T. Chow, 1990a. Free vibration analysis of rectangular plates using orthogonal plate function. Computers and Structures, 34: 79-85.

Liew, K.M. and K.Y. Lam, 1990b. Application of two-dimensional orthogonal plate function to flexural vibration of skew plates. J. Sound Vibrat., 139: 241-252.

Liew, K.M. and K.Y.A. Lam, 1991. Rayleigh-Ritz approach to transverse vibration of isotropic and anisotropic trapezoidal plates using orthogonal plate functions. Intl. J. Solids Structures, 27: 189-203.

Liew, K.M., 1992a. Vibration of symmetrically laminated cantilever trapezoidal composite plates. Intl. J. Mech. Sci., 34: 299-308.

Liew, K.M., 1992b. A hybrid energy approach for vibration modeling of laminated trapezoidal plates with point supports. Intl. J. Solids Structures, 29: 3087-3097.

Liew, K.M. and K.Y. Lam, 1992. Vibrational response of symmetrically laminated trapezoidal composite plates with point constraints. Intl. J. Solids and Structures, 29: 1535-1547.

Liew, K.M. and M.K. Lim, 1993. Transverse vibration of trapezoidal plates of variable thickness: Symmetric trapezoids. J. Sound Vibration, 165: 45-67.

Liew, K.M., 1994. Vibration of clamped circular symmetric laminates. ASME J. Vibrat. Acoustics, 116: 141-145.

Liew, K.M. and M.K. Lim, 1994. Transverse vibration of trapezoidal plates of variable thickness: Unsymmetric trapezoids. J. Sound Vibrat., 177: 479-501.

Linjama, J. and T. Lahti, 1992. Estimation of bending wave intensity in beams using the frequency response technique. J. Sound Vibrat., 153: 21-36.

Linjama, J., 1994. Propagation of mechanical vibration in structure, experimental development of the vibration intensity method, VTT Publication 170. Technol. Res. Centre of Finland.

McFarland, D.E., 1967. An investigation of the elastic stability of corrugated rectangular plates loaded in pure shear, Ph. D Thesis, University of Kansas, USA.

Mandal, N.K., M.S. Leong and R. Rahman, 2000. Measurement of quasi-longitudinal wave power in thin single-layer naturally orthotropic plates. Intl. J. Acoustics Vibrat., 5: 106-108.

Mandal, N.K., R. Rahman and M.S. Leong, 2002. Prediction of Structure borne sound in orthotropic plates for far field conditions. J. Vibrat. Control, 8: 3-12.

Mandal, N.K., R. Rahman and M.S. Leong, 2003. Structure-borne power transmission in thin naturally orthotropic plates: General case. J. Vibrat. Control, 9: 1189-1199.

Mandal, N.K., R. Rahman and M.S. Leong, 2004. Determination of damping loss factors of corrugated plates by the half-power bandwidth method. Ocean Eng: An Intl. J. Res. Develop., 31: 1313-1323.

Mandal, N.K., R. Rahman and M.S. Leong, 2005. Experimental Investigation of vibration power flow in thin technical orthotropic plates by the method of vibration intensity. J. Sound Vibrat., 285: 669-695.

Mead, D.J., 1982. Noise and Vibration, Chapter 25, Vibration Control I, White, R.G. and J.G. Walker (Eds.). England, Ellis Horwood Ltd.

Noiseux, D.U., 1970. Measurement of power flow in uniform beams and plates. J. Acoustical Soc. Am., 47: 238-247.

Quinlin, D., 1985. Application of the four-channel technique to the measurement of power flow in structures, Proceeding of the Second International Congress on Acoustic Intensity, CETIM, Senlis, France, pp: 227-234.

Pavic, G., 1976. Measurement of structure borne wave intensity, Part I: Formulation of the methods. J. Sound Vibrat., 49: 221-230.

Shibata, K., M. Kato, N. Takatsu, O. Wakatsuki and K. Kobayashi, 1994. Measuring condition and precision of structural intensity. Proc. Inter-Noise, 94: 1697-1700.

Szilard, R., 1974. Theory and Analysis of Plates: Classical and Numerical Methods, New Jursey, Englewood Cliffs.

Tanaka, N., 1996. Vibration and acoustic power flow of an actively control thin plate. Noise Control Eng. J., 44: 23-33.

Troitskey, M.S., 1976. Stiffened Plates: Bending, Stability and Vibration, Elsevier, Amsterdam.

Timoshenko, S.P., 1959. Theory of Plate and Shells, Auckland, MaGrawHill Book Company.

Ugural, A.C., 1981. Stress in Plates and Shells, New York: McGrawHill.

Verheij, J.W., 1980. Cross-spectral density methods for measuring structure borne power flow on beams and pipes. J. Sound Vibrat., 70: 133-138.

Xu, X.D., H.P. Lee and C. Lu, 2005. Power flow paths in stiffened plates. J. Sound Vibrat., 282: 1264-1272.

Zhang, Y. and J.A. Mann III, 1996. Example of using structural intensity and the force distribution to study vibrating plates. J. Acoustical Soc. Am., 99: 354-361.